

GENERALIZATION OF CHANNEL BLOCKAGE PROFILES FOR SATCOM ON-THE-MOVE USING 3-D MODELS

Matthew D. Brennan, W. Mark Smith
MIT Lincoln Laboratory
244 Wood Street, Lexington, MA 02420
mattb@ieee.org, wmsmith@ll.mit.edu

ABSTRACT

An extensive measurement campaign was carried out in the fall of 2004 to characterize the EHF SATCOM on-the-move (OTM) channel. Although the measurement locations included many types of terrain and covered a large geographical area, the elevation angle to the satellite was essentially the same throughout the campaign. In this paper we use a 3-D model to extend the results of our previous campaign for arbitrary satellite locations.

INTRODUCTION

The satellite channel in a SATCOM on-the-move (OTM) system experiences outages due to channel blockage by buildings, trees, and other obstructions in the environment. An extensive measurement campaign was conducted in the fall of 2004 to characterize this channel in a variety of locations and operating conditions.

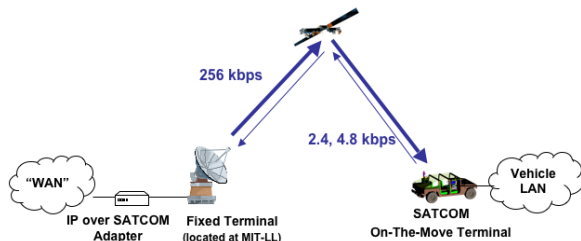


Fig. 1. Experiment configuration.

The experiment setup for the channel measurements described in [1] is shown in Fig. 1. The configuration consists of a control center with a server that provides data flows to a HMMWV over a satellite communication channel. The forward link supports a medium data rate (MDR) 256 kbps downlink to the vehicle. The return link to the control center supports low data rate (LDR) channels running at either 2.4 or 4.8 kbps. The strength

This research was sponsored by the Department of the Army under Air Force Contract FA8721-05-C-0002. Opinions, interpretations, conclusions, and recommendations are those of the authors and are not necessarily endorsed by the United States Government.

of the 20 GHz downlink signal is used to characterize the channel. The output of an energy estimator in the demodulator is used as a signal strength metric. The signal strength measurement is used to construct models for various operating environments.

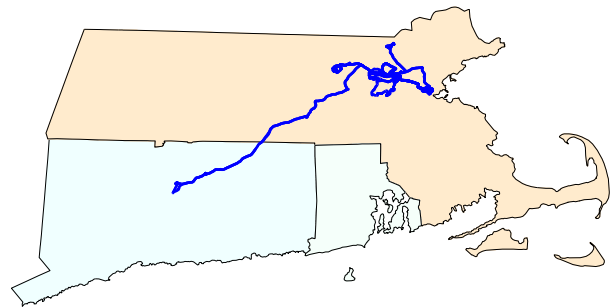


Fig. 2. Measurement locations for the 2004-2005 measurement campaign.

There are, however, limitations to these data sets and the models that are derived from them. The areas covered by the measurement campaign are shown in Fig. 2. All of the measurements are taken from the same satellite at locations that were within about 0.6° of latitude and 1.6° of longitude. As a result, the measurements and models may be biased to these operating conditions. Measurements using satellites at different locations in the sky are needed to generalize the results.

There are fewer satellites available than points of interest in the sky for development of a generalized blockage model. In this paper we use a three-dimensional model of the buildings in Boston, MA, to estimate outage locations. Because multipath reception is essentially eliminated by the highly directional SATCOM antenna, optical methods are used to determine outage locations for ground nodes. These shadowed locations are compared to measurements made in Boston during the previous measurement campaign. The channel blockage statistics obtained through measurement and simulation are also compared.

Using the verified simulation model, outage profiles are determined for arbitrary points along the satellite's

orbital arc. These simulations are used to generalize the blockage channel model for different elevation angles.

PREVIOUS WORK

Different approaches have been used in the past to model the SATCOM OTM channel. Loo and Butterworth [2] give an overview of modeling envelope and phase variations for the channel. Abdi *et. al.* [3] and Dovis *et. al.* [4] introduce new statistical small-scale fading models, while Döttling *et. al.* [5] and Oestges and Vanhoenacker-Janvier [6] take a more deterministic approach with ray-tracing.

Markov models are appealing because of their simplicity and their ability to model a fundamental change in state of the underlying system. Gilbert [7] uses Markov models to describe the behavior of burst errors on a telephone line. Similarly, the loss of signal strength from the satellite in a SATCOM OTM system results in bursts of errors when decoding the received signal.

More recently, others [8]–[11] have had reasonable success in modeling the SATCOM on-the-move channel as being in states with two or three degrees of freedom governed by Markov models. Schodorf [8] models the channel state using a simple two-state Markov model and an augmented Gilbert-Elliot model. We use the two-state Markov model described by [8] for comparisons between measurements and the simulations used in this paper.

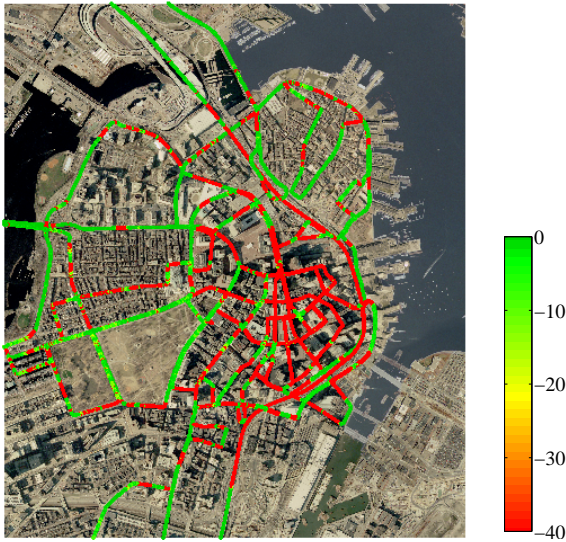


Fig. 3. Measurements in Boston, MA.

SIMULATION OVERVIEW

Figure 3 shows the results of measurements made in Boston, MA. Each measurement location is denoted by a colored point plotted on the overhead image. The color corresponds to signal strength in dB relative to

power received when nothing is blocking the path to the satellite.

From the visual depiction of signal strength, one can immediately see the impact that the density of buildings has on the availability of the communications channel. Close inspection of the data shows that the locations are accurate enough to exhibit repeated blockage by the same buildings when streets are traveled multiple times. Measurements in and around the Boston financial district clearly exhibit blockage effects that are dominated by buildings in these areas.

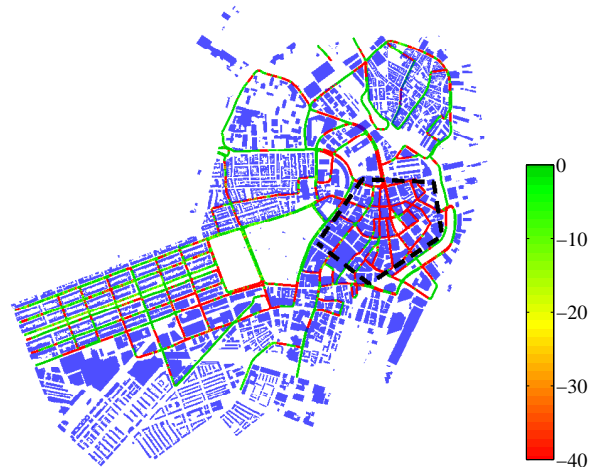
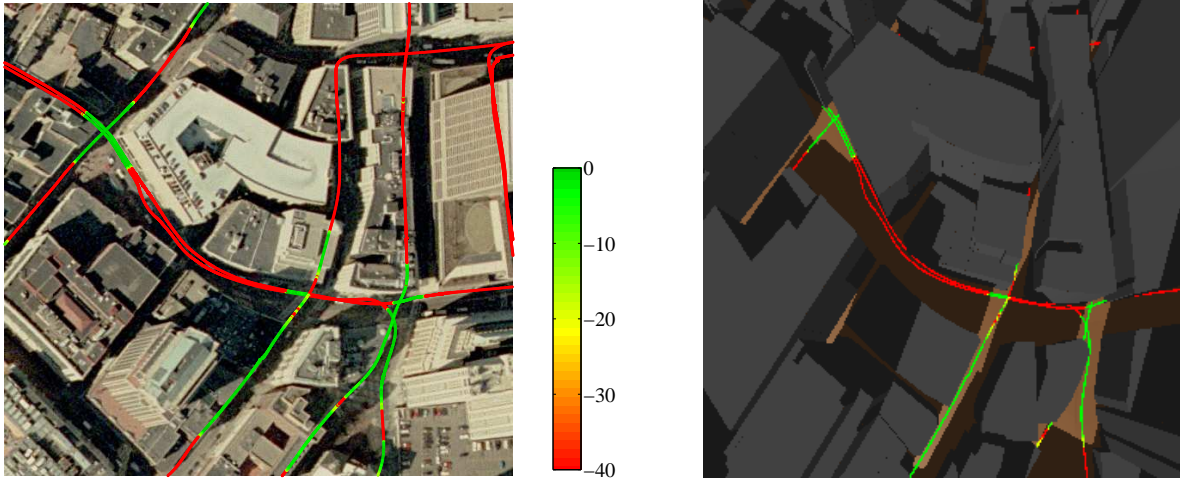


Fig. 4. Model area and corresponding measurement locations. The financial district is enclosed in a black dashed pentagon.

Because the presence of buildings in the environment is a reliable indicator of blockages in the recorded data, we use a three-dimensional model to predict where outages should occur for arbitrary satellite locations. We use a commercial 3-D model obtained from The Sanborn Map Company. Heights in the model are accurate to within 3 ft for at least 90% of buildings. The buildings that make up the model are shown alongside the corresponding physical measurements in Fig. 4. The model covers the buildings in the city of Boston and in the Back Bay neighborhoods.

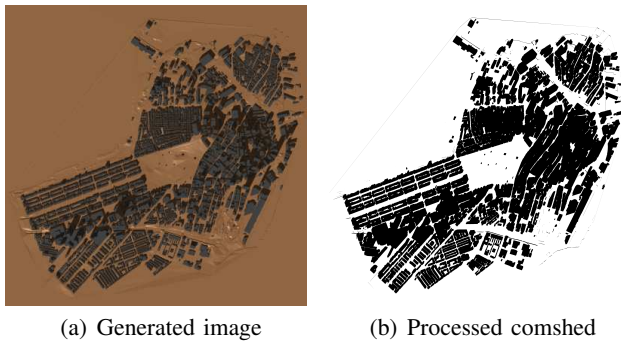
Figure 5 compares measurements and simulation results for a small region in the financial district. Figure 5(b) was generated using the POV-Ray ray-tracing program [12]. The buildings were constructed from the commercial model and placed onto the Massachusetts Standard State Plane, which uses a Lambert Conformal Conic projection [13]. We add ground heights to the plane, which are obtained from the same commercial data set. Six feet are taken from each building height to compensate for the height of the satellite antenna above the ground. A light source is placed at 206.3° from north at an elevation angle of 36.7° . These correspond to the



(a) Close-up view of measurements in the Boston financial district

(b) 3-D blockage model example

Fig. 5. Comparison between measurements and simulation.



(a) Generated image

(b) Processed comshed

Fig. 6. Comshed images.

average look angle for the measurement data. We note here that, due to atmospheric refraction, the look angle differs from the geometric angle to the satellite [14]. The shadow regions projected onto the ground surface correspond to the predicted outage intervals.

We first confirm the 3-D model by qualitatively comparing the model's shadow regions to blockages recorded in the measurement data. Figure 5(a) shows a close-up view of a region in the financial district. The measurement points are superimposed on the overhead image. Modeled versions of the buildings in Fig. 5(a) are shown in Fig. 5(b).

ANALYSIS

Validity of the simulation model comes from a comparison of the blockage statistics. Our POV-Ray model uses an orthographic projection with anti-aliasing turned off to get Fig. 6(a). The orthographic projection uses parallel traces to eliminate perspective. Anti-aliasing is turned off to prevent blurring of shadows' edges. At

the resolution chosen, each pixel represents a 2×2 ft area. From this image, a comshed is generated based on each pixels RGB color values. For our purposes, a comshed is a 2D binary matrix indicating where on a plane the SATCOM channel is open or blocked. This is shown graphically in Fig. 6(b). From this comshed, we deterministically find the channel to be either open or blocked. For comparison, blockage state of the measured data is found by thresholding samples at our approximate SNR margin of -5 dB, as shown in Fig. 7.

Along the paths travelled, we find the simulated blockage state at the point of each real measurement taken. Next, spatial lengths of continuously open and blocked channel state are measured. Distance between measured points is based on the measurement's latitude and longitude on the GRS80 spheroid [13]. The state change follows a hysteresis rule: when the current measurement or simulation differs from the previous state, we change if a majority of the next 10 points agree with the new state. Since there are multiple measurements per representative pixel, this has the general effect of removing temporal variation in the measurement signal, and has little effect on the simulated channel state.

The empirical complementary cumulative distribution function (ccdf) is then computed for open and blocked state lengths. Plots of these functions for both measurement and simulation are shown in Figs. 8(a) and 8(c) on semi-log axes. The simulated functions are a close approximation to the functions for actual measurements.

The data set that describes Boston consists of two different regions. The financial district contains a dense urban core of tall, closely spaced buildings. This area is highlighted in Fig. 4. Outside this core are areas

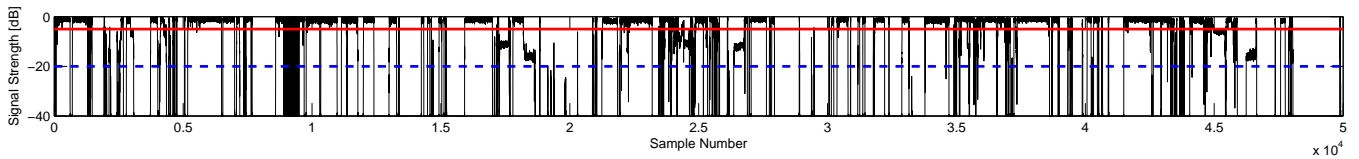


Fig. 7. A subset of measured signal strengths. The red solid and blue dash lines are -5 dB and -20 dB, respectively.

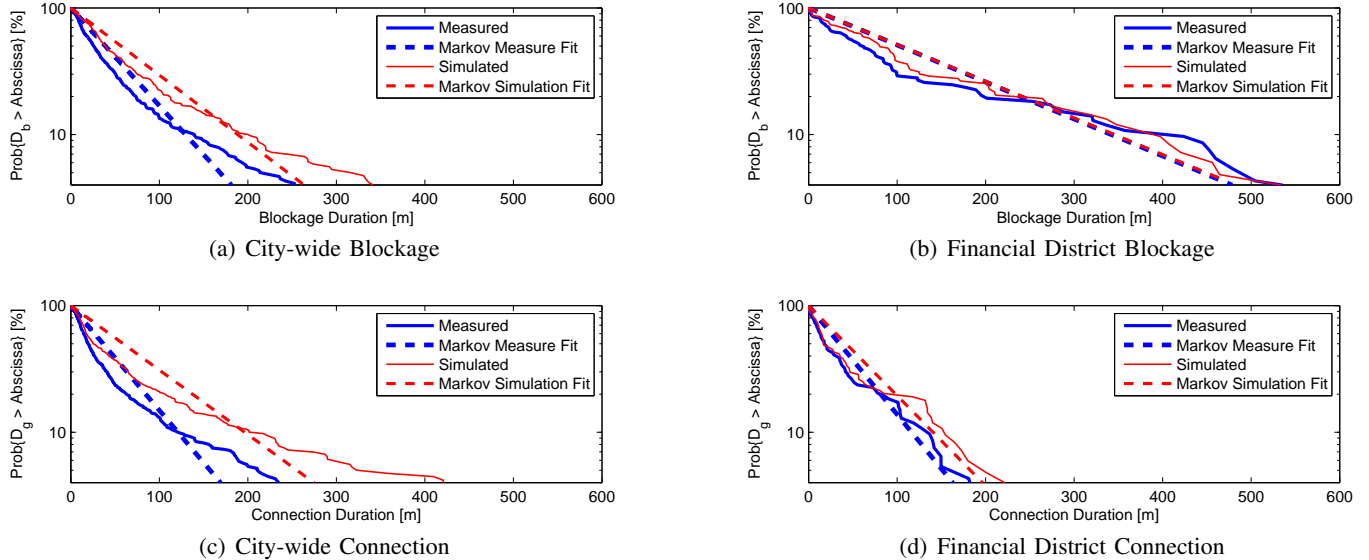


Fig. 8. Complementary cumulative distribution functions and channel estimations for measurements in Boston, MA.

with lower building densities and more vegetation. Due to the high density of tall buildings in the financial district, the distributions for the data in this region are different from the distributions for the entire city, as reflected in Fig. 8. Additionally, since the environment in the financial district is dominated by structures that are included in our model, simulation results are a closer match to measurements.

Through pointwise comparison of the simulation and measurements for the whole city, taking distance between points into account as before, we find that 82.3% of the simulation matches the measurements. Close inspection of results shows clear explanations for some of the errors.

A. Instantaneous satellite position

For our simulations, we take the satellite position as fixed at its average location. In reality, however, during measurements the satellite had a total variation of 2.2° in azimuth and 5.2° in elevation due to diurnal variation of the inclined orbit. Simulating these extremes in addition to the average, we find 85.4% of the measurements are matched in at least one case. Figure 9 is a histogram of

error lengths which cannot be explained by the satellite position.

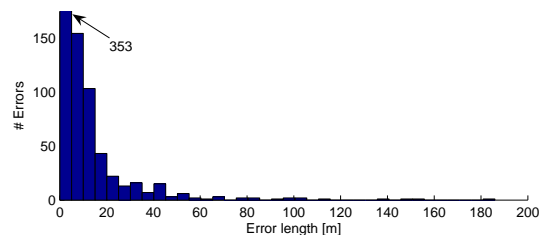


Fig. 9. Histogram of error lengths for -5 dB threshold.

B. Building model

Building positions are measured from the ground for this model, and are expected to be accurate. Building heights, however, are based on aerial photography, and are therefore relatively imprecise. As stated above, only 90% are guaranteed accurate to within 3 ft per the Sanborn specification. While we believe the actual error may be less than this in general, it remains significant. Additionally, buildings are approximated to have flat roofs. While this a good approximation for some buildings, many throughout the city have slanted roofs. Height

for these buildings is taken as the average, which may cause a poor approximation of the shadowing. In Fig. 10 agreement and disagreement between measurements and simulation are plotted in green and red respectively. The two long sections of mismatch in Fig. 10(b) demonstrate how minor error in building height could potentially cause significant mismatch.

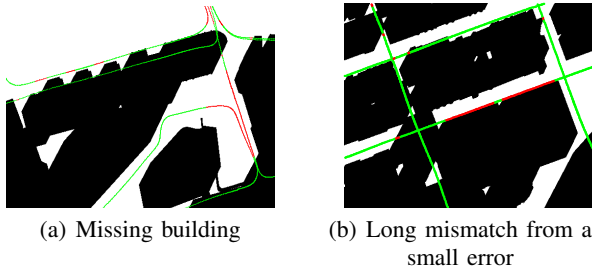


Fig. 10. Select errors. Red represents difference between simulation and measurement. Green represents agreement.

Two other errors are shown in Fig. 10(a). Both are longer than 90 m, and the result of our model missing a particular building. While the building model was generated in August of 2002, measurements of this area were not taken until November of 2004. Imagery taken at the same time as the model reveals a construction site. It is not clear which other buildings may also have changed during this time.

C. Foliage

At 20GHz, trees are a significant obstacle to RF propagation [1, 8]. The large areas without buildings in Fig. 11 are the Boston Common and Public Garden. This area is dominated by vegetation rather than building structure. The Back Bay, to the left of the commons, also has large amounts of foliage in some areas. The large number of mismatches around these areas can be explained by the presence of this vegetation.

Figure 11(a) uses measurements thresholded at the previously mentioned -5 dB level. For comparison, Fig. 11(b) uses -20 dB. While there is little difference in areas of dense buildings, areas with foliage are quite dissimilar. Portions of the model not shown in these figures contain dense buildings, and demonstrate high levels of matching.

D. Measurement coordinates

Measurement coordinates are taken from an inertial navigation system. This system maintains accurate differential position. Absolute position is obtained from a GPS unit, which exhibits occasional errors. While recorded measurement locations generally

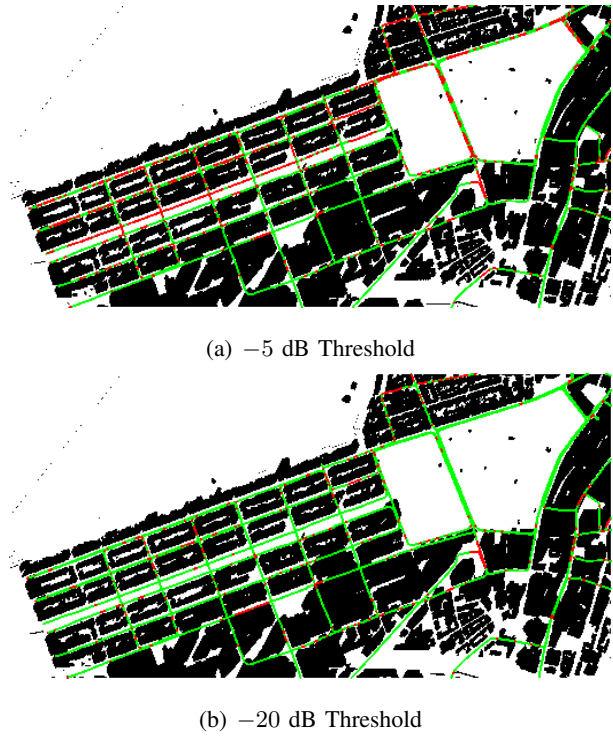


Fig. 11. Errors in Back Bay and Commons for different thresholds. Red represents difference between simulation and measurement. Green represents agreement.

corresponded to streets, as expected, one section was off by around 10 m. A 1km section was corrected manually, as shown in Fig. 12. While this error was obvious, errors of less than a meter would not be noticeable, and may be an alternate explanation for mismatches like that of Fig. 10(b).

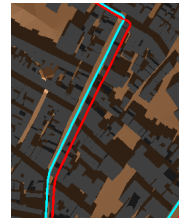


Fig. 12. Measured and corrected paths are shown in red and blue, respectively.

E. Road structures

Roadways also have an effect on the OTM channel. One section of outage was removed from our analysis once identified as measurements inside a tunnel. While not a factor in the subset of data analyzed here, we note that other areas of Fig. 2 showed effects from traveling below elevated roadways. For a complete model, these structures must also be considered.

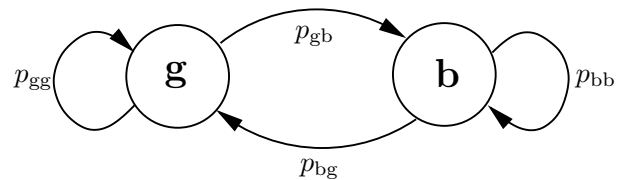


Fig. 13. The two-state Markov model.

CHANNEL GENERALIZATION

To model the channel, we use the simple two-state Markov process used by Schodorf [8], which is shown in Fig. 13. The model represents two states: a “good” state \mathbf{g} denoting error-free communication and a “bad” state \mathbf{b} in which communication is lost. We find parameter p_{gg} by fitting the measured ccdf to the ccdf for open channel duration in the two-state Markov model,

$$\text{prob}\{D_g > n\} = p_{gg}, \quad (1)$$

where n represents the spatial duration. p_{bb} is found analogously with the blocked channel duration. The estimated blockage fraction, π_b , is given as [8]

$$\pi_b = \frac{p_{gb}}{p_{gb} + p_{bg}} \quad (2)$$

where $p_{gb} = 1 - p_{gg}$ and $p_{bg} = 1 - p_{bb}$.

The values for p_{gg} and p_{bb} are plotted in Fig. 8 as dashed lines. We find that, for our data, the quality of this model’s fit varies with the nature of the environment. The financial district of Boston exhibits a very close fit for both the connected and blocked durations, as shown in Figs. 8(b) and 8(d). Both measured and simulated statistics for the whole city, shown in Figs. 8(a) and 8(c), have considerable variation from the Markov generalization. This is primarily caused by a heavier weight towards short durations, which is usually an indication of foliage.

Models with additional degrees of freedom have been used in previous works. In [9], Bråten and Tjelta use a semi-Markov model, while Schodorf uses a Gilbert model in [8]. These models are outside the scope of this work.

VARYING SATELLITE POSITION

We use the geostationary orbital arc, shown in Fig. 14, as viewed from Boston to sample alternate satellite locations. Sampled positions along the arc were run through the simulation and generalization procedures. Using the same measured path as before, Fig. 15 shows ccdf’s and Markov model parameters for several of these simulations. The colors of the sample locations in Fig. 14 correspond to the colors of the curves in Fig. 15.

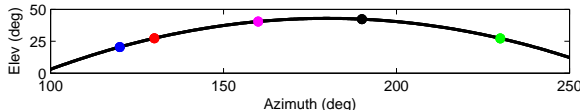


Fig. 14. Orbital arc used for simulations.

The differences between Figs. 15(a) and (b) again highlight characteristics of their respective areas. Connected durations in the densely built financial district are

considerably shorter than both financial district blocked duration and city-wide open duration. Also reinforced from earlier is that the model has closer fit to data for the financial district. The fit is also close for the connected duration in the city. Only city-wide blockage duration has a poor fit.

Figure 16 shows simulated parameters found along the parabola. Plots for π_b are labeled as parameters, since derived from p_{gg} and p_{bb} . Plots labeled “actual” are simulated blockage fractions measured pointwise, taking distance into account as before. We note that the derived π_b appears to be an accurate measurement of the blockage fraction. The sharp drops in p_{gg} occur when the area is entirely blocked. This drop is evident in the financial district for low elevation angles.

The city-wide plots in particular demonstrate the significance of the satellite azimuth relative to building orientation for the OTM channel. For example, at 15° of elevation, π_b has values near either 55% or 80%: a non-trivial difference. For our dataset, this variance is largely due to the regular layout of buildings in the Back Bay area relative to the look angle to the satellite.

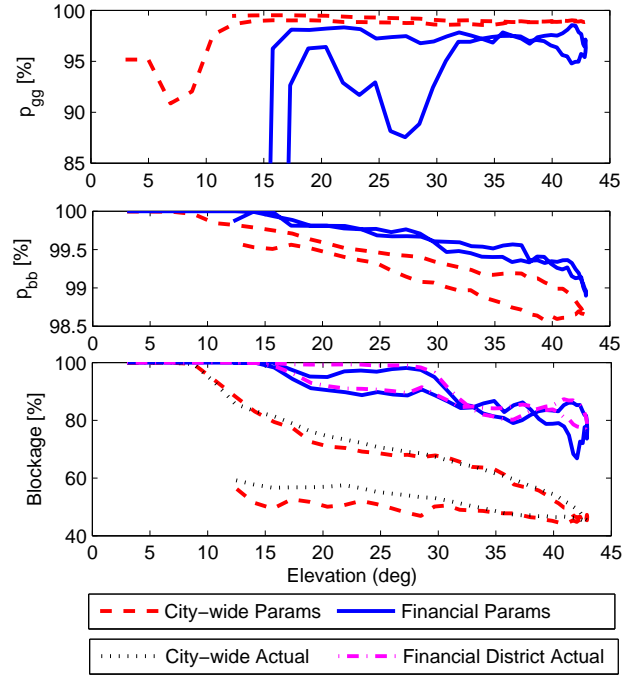


Fig. 16. Simulated p_{gg} , p_{bb} and blockage vs. satellite look elevation. For blockage, π_b is a derived value, labeled as a parameter value. “Actual” is obtained from pointwise measurement in the simulation

SUMMARY

Using a commercial three-dimensional building model, we have generalized the OTM channel for urban and dense urban areas with arbitrary satellite locations.

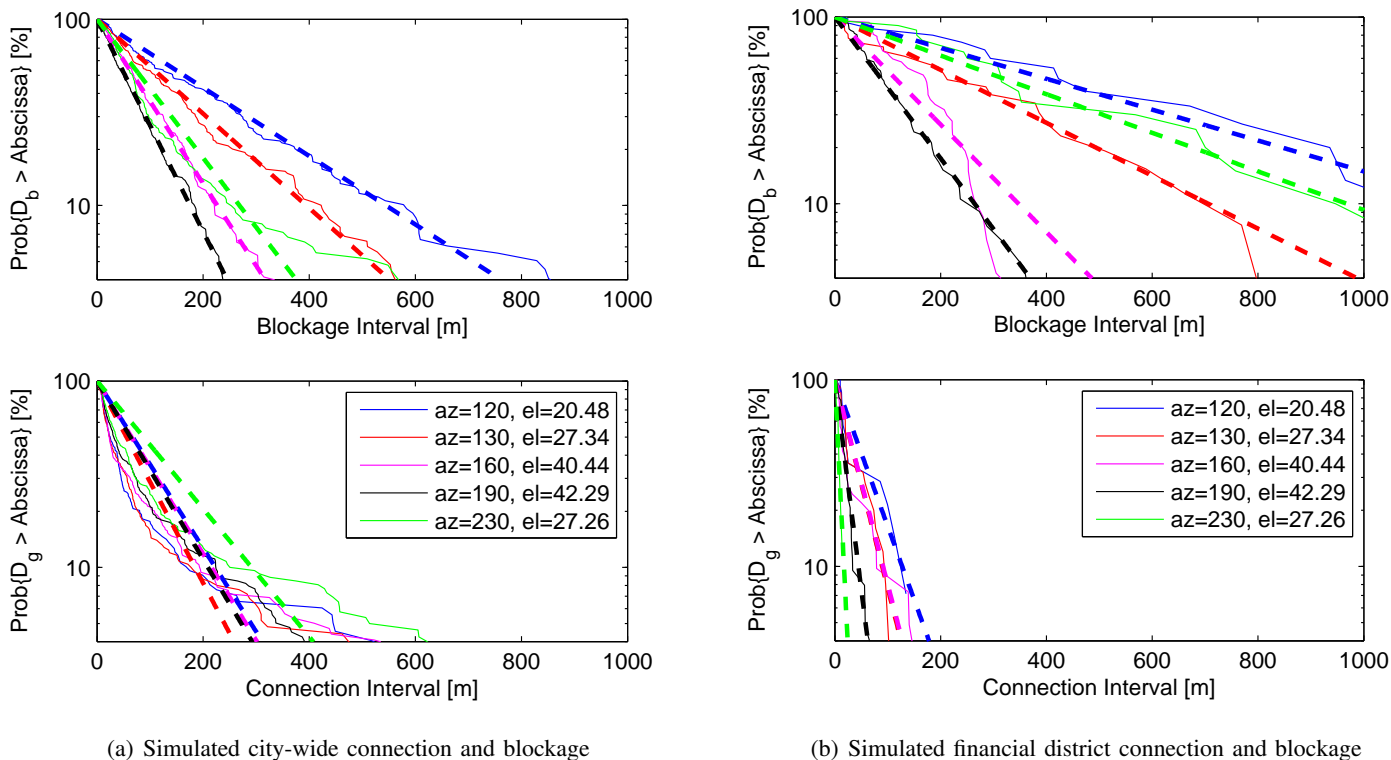


Fig. 15. Simulations for arbitrary satellite locations.

We have shown that ray-tracing provides an accurate simulation model when an area is dominated by buildings and that foliage and other obstructions are critical in less dense areas. From analysis of the different matches for thresholds of -5 and -20 dB, we believe that deterministic ray-tracing may be effective using solid foliage models, but that more data is necessary to demonstrate this.

We have also shown that simple Markov models can provide good approximation for some environments. It is clear, however, that models containing additional degrees of freedom are often required to obtain more accurate fits to the data.

REFERENCES

- [1] W. M. Smith, "Channel characterization for EHF satellite communications on the move," MIT-LL, Tech. Rep. TR-1109, Jul. 2006.
- [2] C. Loo and J. S. Butterworth, "Land mobile satellite channel measurements and modeling," *Proceedings of the IEEE*, vol. 86, no. 7, pp. 1442 – 1463, 1998.
- [3] A. Abdi, W. C. Lau, M.-S. Alouini, and M. Kaveh, "A new simple model for land mobile satellite channels: first- and second-order statistics," *IEEE Transactions on Wireless Communications*, vol. 2, no. 3, 2003.
- [4] F. Dovis, R. Fantini, M. Mondin, and P. Savi, "Small-scale fading for high-altitude platform (HAP) propagation channels," *IEEE Journal on Selected Areas in Communications*, vol. 20, no. 3, pp. 641 – 647, 2002.
- [5] M. Dottling, A. Jahn, D. Didascalou, and W. Wiesbeck, "Two- and three-dimensional ray tracing applied to the land mobile satellite (LMS) propagation channel," *IEEE Antennas and Propagation Magazine*, vol. 43, no. 6, pp. 27 – 37, 2001.
- [6] C. Oestges and D. Vanhoenacker-Janvier, "Propagation modeling and system strategies in mobile-satellite urban scenarios," *IEEE Transactions on Vehicular Technology*, vol. 50, no. 2, pp. 422 – 429, 2001.
- [7] E. N. Gilbert, "Capacity of a burst-noise channel," *Bell Sys. Tech. J.*, pp. 1253 – 1265, Sep. 1960.
- [8] J. B. Schodorf, "EHF satellite communications on the move: Experimental results," MIT-LL, Tech. Rep. TR-1087, Aug. 2003.
- [9] L. E. Braten and T. Tjelta, "Semi-Markov multistate modeling of the land mobile propagation channel for geostationary satellites," *IEEE Transactions on Antennas and Propagation*, vol. 50, no. 12, 2002.
- [10] F. P. Fontan, M. Vazquez-Castro, C. E. Cabado, J. P. Garcia, and E. Kubista, "Statistical modeling of the LMS channel," *IEEE Transactions on Vehicular Technology*, vol. 50, no. 6, pp. 1549 – 1567, 2001.
- [11] H. Yao, "EHF satellite communications-on-the-move: Blockage channel modeling," MIT-LL, Tech. Rep. TR-1098, Nov. 2004.
- [12] "POV-Ray," <http://www.povray.org/>, Persistence of Vision ray-tracing program.
- [13] J. P. Snyder, *Map Projections — A Working Manual*. Washington, DC: US Government Printing Office, 1987.
- [14] J. E. Allnutt, *Satellite-to-Ground Radiowave Propagation*. London, United Kingdom: Peter Peregrinus Ltd, 1989.